scientific reports

Check for updates

OPEN

A novel method for isolation of tumor infiltrating myeloid-derived suppressor cells from human lung tumor tissue

Marta Piqueras-Nebot[1,6], Marta Benet[1,6], Miriam Estors[2], Antonio Cremades[3], Óscar Juan-Vidal[1,4], Julián Carretero[5], José Marcelo Galbis-Caravajal[2] & Agustín Lahoz[1]✉

The tumor microenvironment comprises different cell subsets including myeloid-derived suppressor cells, which exert intratumoral immunosuppression and favor cancer progression. Isolating tumor-infiltrating myeloid-derived suppressor cells (tMDSCs) from human tumor samples remains a challenge. Current methods such as magnetic bead sorting (MACS) or flow cytometry sorting (FACS) present some drawbacks in terms of purity and viability. Here, we have setup an innovative workflow that combines RosetteSep technology and MACS for isolation of tMDSCs from lung cancer biopsies. To evaluate our Rosette-MACS approach, we compared its performance with MACS and FACS. The isolated cells were characterized by flow cytometry, gene expression analysis and proliferation assays for comparison purposes. The results showed that the Rosette-MACS protocol had the highest yield and purity of tMDSCs (79.64% vs 13.30% with FACS and 0.39% with MACS). Furthermore, the functionality of the isolated tMDSCs was tested not only by upregulation of immunosuppressive genes (e.g. *ARG1*, *IDO1*, or *PD-L1*), but also by their capacity to inhibit CD8⁺ T cells proliferation. The combined use of RosetteSep and MACS provides an improved approach for the isolation of functional tMDSCs, which delineates a suitable experimental framework to selectively study the molecular mechanisms underpinning tMDSCs-derived immunosuppression in the TME.

Keywords Myeloid-derived suppressor cells, Human, Tumor-infiltrating, Isolation, Lung cancer, Immunosuppression

The tumor microenvironment (TME) is a complex and eclectic ecosystem in which different cell subsets interact, including cancer, stroma, endothelial cells but also heterogeneous host cells of the immune system, which collectively shape the disease course[1,2]. Among the tumor-infiltrating leukocytes, effector cells such as natural killer (NK) cells or cytotoxic $CD8^+$ T lymphocytes activate a powerful tumor-fighting immune response that is able to restrain tumor growth[3]. Conversely, the aberrant expression of tumor-derived soluble factors such as chemokines, growth factors and inflammatory cytokines drive an "emergency" myelopoiesis, leading to the pathological differentiation of myeloid lineage into alternatively pro-tumorigenic cells, mainly represented by tumor-associated macrophages (TAMs) and myeloid-derived suppressor cells (MDSCs), which exert intratumoral immunosuppression and favour tumor progression[4,5]. MDSCs are a heterogenous group of immature immunosuppressive myeloid cells that rapidly expand in response to pathogenic infections, cancer, inflammation, trauma or autoimmune disease[6]. MDSCs are conventionally classified into two major subpopulations: polymorphonuclear (PMN-MDSCs) and monocytic (M-MDSCs). Phenotypically, human PMN-MDSCs are defined as $CD33^+CD11b^+$ HLA-$DR^{low/-}CD15^+CD14^-$, while M-MDSCs as $CD33^+CD11b^+$HLA-$DR^{low/-}CD15^-CD14^+$[7,8]. However, it is still very challenging to discriminate immunosuppressive PMN- and M-MDSCs from their pro-inflammatory counterparts (neutrophils and monocytes, respectively) as they share cellular origin and phenotypic and morphological markers, although they have different biologic signatures[4,6]. In humans, M-MDSCs could be separated from monocytes based on the expression of MHC class II molecule-

[1]Biomarkers and Precision Medicine Unit, Instituto de Investigación Sanitaria La Fe, 46026 Valencia, Spain. [2]Thoracic Surgery Service, Hospital Universitario de La Ribera, Valencia, Spain. [3]Pathological Anatomy Service, Hospital Universitario de La Ribera, Valencia, Spain. [4]Medical Oncology Service, Hospital Universitario y Politécnico La Fe, Valencia, Spain. [5]Phisiology Department, University of Valencia, Valencia, Spain. [6]Marta Piqueras-Nebot and Marta Benet contributed equally to this work. ✉email: agustin.lahoz@uv.es

HLA-DR. Until recently, the only method allowing the separation of neutrophils from PMN-MDSCs in humans was gradient centrifugation using a standard Ficoll gradient. PMN-MDSCs are enriched in the low-density fraction (PBMCs), whereas neutrophils are high density cells. Recently, the expression of Lectin-type oxidized LDL receptor 1 (LOX-1) is specifically detected in PMN-MDSCs[9,10]. Circulating, splenic and tumor-infiltrating MDSCs (tMDSCs) differ in gene expression profiles[11], metabolism[12] and in the levels of key immune controlling proteins such as PD-L1[13]. In the TME, tMDSCS contribute to tumor progression through non-immunological functions, including promoting angiogenesis through the VEGFA/COX2 axis and contributing to metastasis of tumor by inducing a mesenchymal phenotype and the formation of the pre-metastatic niche[14–16]. tMDSCs inhibit adaptive antitumor immunity by suppressing T-cell effector functions in the TME through a range of mechanisms, such as arginase 1 (ARG1)- and nitric oxide synthase 2 (NOS2)- mediated depletion of L-arginine; tryptophan catabolism into kynurenines by indoleamine 2,3-dioxygenase 1 (IDO1) or the restriction of the extracellular pool of cysteine[1,4,17]. All these data together suggests that tMDSCs delineates a more appropriate model to study the role of MDSCs within the TME than other sources of MDSCs. Despite their critical role in tumor immunology, the isolation and characterization of tMDSCs from human tissues, particularly in solid tumors such as non-small cell lung cancer (NSCLC), remain challenging. Different commercial kits have been developed to enrich tMDSCs from murine tissues (EasySep™ Mouse MDSCs (CD11b + Gr1 +) Isolation Kit from Stemcell Technologies or Myeloid-Derived Suppressor Cell Isolation Kit from Miltenyi Biotec). However, there are no kits available for MDSCs isolation from human tumor specimens. Most of previous studies have used two basic isolation kits based on magnetic bead sorting (MACS) or on flow cytometry sorting (FACS) but these simple isolation protocols are not suited for high purity isolation of functional MDSCs subsets[18–25]. Furthermore, these standard techniques frequently fail to fully isolate and purify these cells, resulting in potential loss of biological information and functional heterogeneity.

The present study aimed to develop a novel procedure designed for the reliable and functional isolation and characterization of MDSCs from human tumor tissue samples. By enhancing the accuracy and efficiency of tMDSCs isolation, this method not only provides a powerful tool for studying their functional roles within the TME, but also could lead to more detailed studies into targeted therapeutic approaches aimed at modulating MDSCs activity in the TME.

Results

Setup of tMDSCs isolation using RosetteSep and MACS combination

The most used technique for the isolation of MDSCs from human samples is FACS, which allows to separate cells based on the expression of multiple surface proteins by means of fluorescence-labelled antibodies. Another standard separation technique is one- or two-step MACS, which despite presenting a less complex method, only a maximum of two markers can be used. Nonetheless, studies based on these two techniques fail to report data regarding purity after MDSCs isolation[19,23,25] or to provide a comprehensive characterization, mainly because they rely on markers such as CD14, CD16 and CD11b[18,26], without considering other key surface markers for MDSCs, such as CD33 or HLA-DR[7,8]. Overall, these two traditional separation techniques involve multiple processing steps, require expensive flow cytometry instrumentation and often result in lower cell recovery due to multiple handling steps. Here we compared these two established isolation protocols with an enrichment method (i.e., Rosette-MACS) that has been previously used for the purification of circulating MDSCs from human peripheral blood samples[27,28], although this is the first work to successfully adapt this protocol for human lung tumor tissue. This method combines the advantages of both density gradient enrichment (RosetteSep™ HLA Myeloid Cell Enrichment Kit (Stemcell, Saint Égrève, France)) and magnetic separation (magnetic microbeads against HLA-DR) into a single-step workflow, reducing processing time and minimizing cell loss. RosetteSep is an immunodensity procedure for the isolation of untouched cells directly from whole blood. The unwanted cells are crosslinked to red blood cells (RBCs) present in the sample by specific antibodies forming dense immunorosettes, which pellet during density gradient centrifugation, leaving untouched and purified target cells at the interface between the plasma and the buoyant density medium. By combining RosetteSep technology with HLA Myeloid Cell Enrichment Cocktail, myeloid ($CD33^+$) cells are enriched from the sample by targeting unwanted cells with Tetrameric Antibody Complexes recognizing CD3, CD8, CD19, CD56 and glycophorin A on RBCs. The problem in adapting the RossetteSep-based procedure to tissue samples is the absence of erythrocytes. To overcome this limitation, we enriched the cell suspension obtained after tumor dissociation with autologous fresh RBCs obtained by Ficoll-Hypaque density gradient centrifugation. The proportion of RBCs/tumor suspension was set to 1:1 in PBS, taking into account that the amount of whole blood that is made up of RBCs (hematocrit) is approximately 50% in human adults. By directly targeting MDSCs in whole tumor digests prior to density gradient separation, this approach enhances recovery while maintaining high purity (Fig. 1A).

Comparison of FACS, MACS and Rosette-MACS approaches

The performance of the Rosette-MACS method was evaluated by comparing its yield, cell viability, purity and protocol duration (n = 6) with those figures obtained by FACS where the population of $CD33^+CD11b^+HLA\text{-}DR^{low/-}$ cells was shorted (n = 4) and with MACS where microbeads against HLA-DR and CD14 were used to obtain the fraction of HLA-DR-CD14 + from 4 tumor tissue cell suspensions (Fig. 1A, Supplementary Fig. 1). The average weight of all the collected samples was 0.663 g and approximately 113×10^6 cells/ per gram of tumor were obtained after tumor dissociation. Considering the three isolation protocols individually, comparable tissue weights were used (0.667, 0.633 and 0.679 g for FACS, MACS and Rosette-MACS, respectively). Noteworthily, the three isolation methods are not biased towards the number of cells/tumor weight (g) obtained after tissue digestion (Fig. 1B). However, the yield differed depending on the separation method applied. The number of tMDSCs recovered with FACS strategy resulted in less than 100,000 cells, which represented less than 1% of

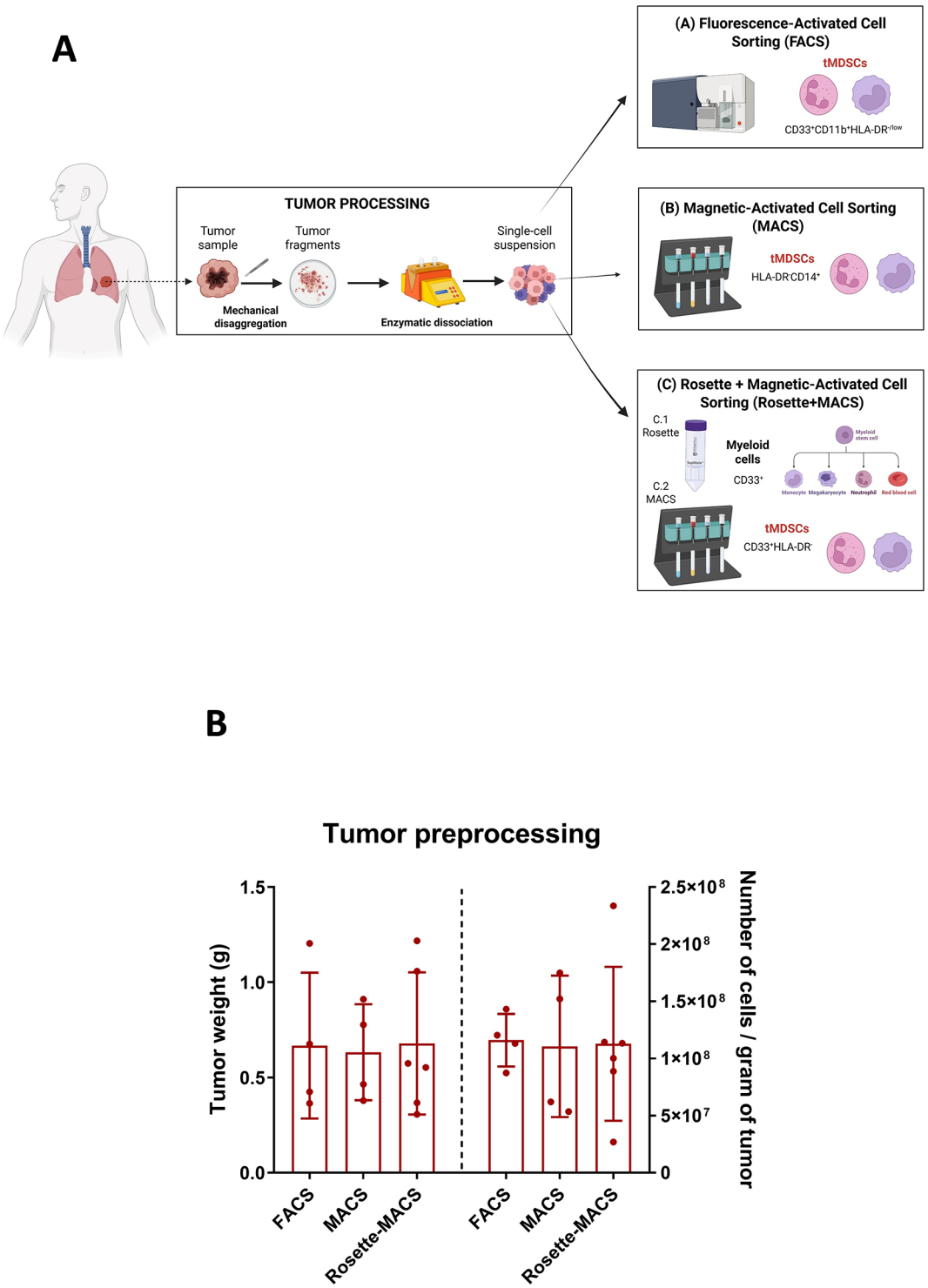

Fig. 1. Lung tumor samples preprocessing for the isolation of tumor-infiltrating myeloid-derived suppressor cells. (**A**) Schematic workflow of the tumor biopsies processing and tMDSCs isolation by three different enrichment methods. (**B**) Comparison of tumor specimen weight and number of cells obtained after tumor dissociation between the three isolation protocols (i.e. FACS, MACS and Rosette-MACS).

the number of initial cells in the tumor suspension. This percentage was the same with MACS technology, although the number of tMDSCs increased up to almost 350,000 cells. The highest recovery was achieved with our proposed protocol (Rosette-MACS), with the number of tMDSCs raising to circa 18,000,000 cells, which corresponded to approximately 40% of the initial sample (Fig. 2A). Further, the greatest cell viability was reached by the Rosette-MACS method (89.33%) compared to the MACS protocol that showed 47.75%. Data of cell viability after FACS sorting was not recapitulated as the cell sorter provided the number of sorted tMDSCs

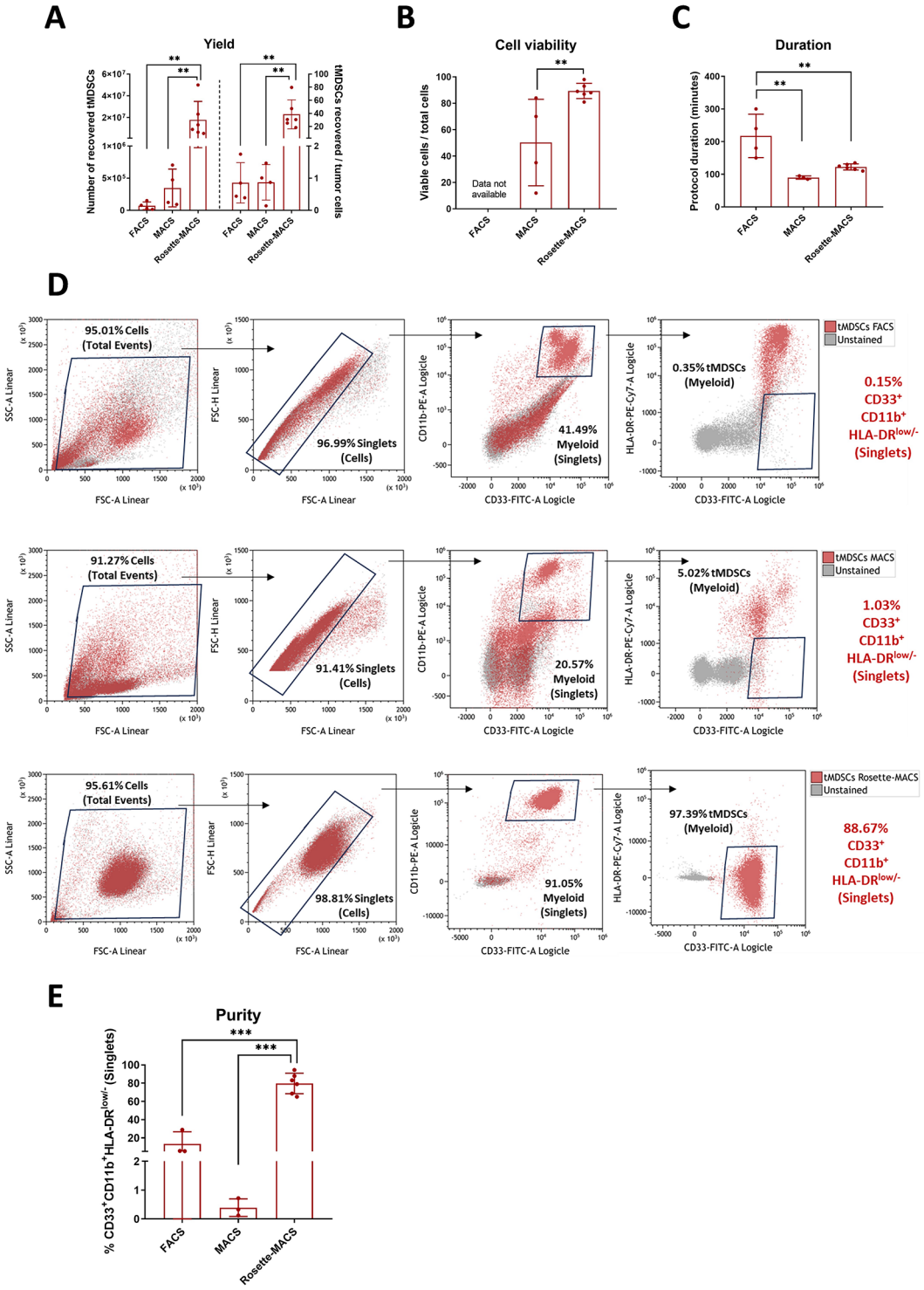

Fig. 2. Comparison of FACS, MACS and Rosette-MACS approaches. (**A**) Yield expressed as number of cells recovered per number of initial tumor cells. (**B**) Cell viability of isolated tMDSCs. (**C**) Duration of each protocol (min). (**D**) Representative flow cytometry biparametric dot plot graphs showing the gating strategy followed to analyse the purity of isolated tMDSCs. (**E**) Purity represented as the percentage of CD33 + CD11b + HLA-DRlow/- cells following the three isolation protocols analyzed by flow cytometry. (**A**–**C**,**E**) Values were mean ± SD, ***p < 0.001 determined by one-way ANOVA.

and no extra cell counting was performed (Fig. 2B). However, it is known that several factors like abrupt and repeated temperature changes, high pressure, shear stress, high voltage electric fields or laser irradiation are present during the cell sorting workflow and can eventually impact viability of sorted cells[29]. On the other hand, according to the manufacturer's protocols, the isolation of tMDSCs by MACS or the combination of RosetteSep

technique and MACS took 90 min and 120 min, respectively. Due to the previous tumor processing steps, the total isolation time of MDSCs from tumor samples by these two enrichment methods accounted to 170 min and 200 min, respectively. The separation of tMDSCs using FACS strategy is more time-consuming, with an average protocol duration of 240 min, without considering the time used for pre-processing of tumor biopsies (Fig. 2C). Isolation of cells by specific CD markers is a reliable method to enrich the cell type of interest and to eliminate contaminating cells. To analyze the purity of the isolated cells we used flow cytometry. Figure 2D shows an example of the flow cytometry analysis performed in our study for determining tMDSCs phenotype after cell isolation. As shown in Fig. 2E, immunophenotypical analysis of tMDSCs revealed that the percentage of $CD33^{+}CD11b^{+}HLA\text{-}DR^{low/-}$ cells obtained after FACS sorting was mostly below 15%, being this value even lower when using MACS technology (0.39%). After separation, the purity of tMDSCs was significantly higher with the Rosette-MACS separation method compared to the FACS and MACS, reaching almost an 80% of $CD33^{+}CD11b^{+}HLA\text{-}DR^{low/-}$ cells, which reinforced the suitability of our novel technique for the isolation of MDSCs from tumor samples.

Altogether, these results show that the new Rosette-MACS present some key advantages over other standard techniques (i.e., FACS and MACS) for tumor-infiltrating MDSCs isolation.

Characterization of tMDSCs isolated by the Rosette-MACS method

Besides purity, functionality of isolated cells is another important factor which is frequently overlooked when evaluating enrichment methods. Here, we evaluated the functionality of isolated tMDSCs following Rosette-MACS protocol by determining the expression of genes related to the immunosuppressive role of these cells and by assessing the proliferation rate of T cells with or without tMDSCs. In relation to gene expression, it is known that MDSCs promote immune suppression and tumor growth and metastasis via the increased expression of coinhibitory (PD-L1) receptors[13], the enhanced pro-inflammatory or pro-angiogenic activity of COX2 and VEGFA[14–16], respectively, or the deprivation of essential metabolites, including arginine and tryptophan, through the upregulation of *ARG1*, *NOS2* and *IDO1* genes[1,4,17]. Therefore, to better characterize the nature of suppressive tMDSCs, gene expression of these putative mechanisms of MDSCs-related suppression was evaluated by quantitative RT-PCR. This analysis indicated that the mRNA level of *ARG1* or *IDO1* was 94-fold and 22-fold, respectively, significantly higher in MDSCs isolated from human lung tumours compared with that of peripheral blood mononuclear cells (PBMCs) isolated from healthy donors (Fig. 3A,B). Furthermore, tumor-infiltrating MDSCs showed 22 and 38 times more significant expression of *PD-L1* and *NOS2* relative to control PBMCs (Fig. 3C,D). Finally, significant induction of gene expression of other immunosuppression-related genes (i.e. *COX2*, *VEGFA, S100A8, S100A9* and *LOX1)* was also observed in tMDSCs compared to control PBMCs (Fig. 3E,I). Besides, the suppressive function of tumor-infiltrating MDSCs obtained with the Rosette-MACS method was also tested by co-culturing freshly isolated MDSCs with CFSE-labelled $CD8^{+}$ T cells isolated from healthy donors that were previously activated with anti-CD3/CD28. After 4 days, T-cell proliferation was assessed by flow cytometry, and it was found that activated $CD8^{+}$ T cells cultured alone showed significantly more proliferation than those cultured with tMDSCs at a ratio 1:2 (57.21% vs 35.03%, $p < 0.05$, $n = 6$; Fig. 3J,K).

Overall, results suggest that the Rosette-MACS protocol does not affect the expression pattern of canonical immunosuppression-related genes and show that tMDSCs remain functional afters isolation, at least, in terms of inhibiting $CD8^{+}$ T-cell proliferation.

Discussion

MDSCs are usually isolated from peripheral blood of cancer patients and rarely, tumor tissue, bone marrow aspirates or splenocytes are used to source MDSCs[30]. Nevertheless, it has been shown that circulating/splenic MDSCs and tumor-infiltrating MDSCs (tMDSCs) are functionally different, most likely due to their different transcriptomic patterns[11], metabolic profiles[12] and expression levels of PD-L1[13]. All these data together point out the importance of establishing protocols for isolation and characterization of human tMDCS specifically since these cells are not only involved in the control of antitumor immune responses, but also in tumor progression. In this sense, MDSCs isolated from peripheral blood of cancer patients cannot be used as a unique model because they do not reflect the real behaviour of tMDSCs and their gene expression patterns differ from their counterparts found in the TME[11]. Moreover, circulating MDSCs display greater plasticity, allowing them to differentiate into other myeloid cell types such as macrophages or dendritic cells. In contrast, tumor-infiltrating MDSCs are more committed to their suppressive roles and show limited plasticity, reflecting their adaptation to the TME[31]. In addition, cancer immunotherapy strategies often target the TME to modulate immune responses effectively and understanding the specific properties of tumor-derived MDSCs is crucial for identifying novel therapeutic targets. In this context, peripheral MDSCs, while informative, may not fully capture the functional landscape of the TME, leading to potential misinterpretations in preclinical and clinical studies.

MACS and FACS are widely used for cell isolation directly from tumor samples but present limitations in the context of isolating MDSCs. Flow cytometry sorting provides the most comprehensive method for isolating MDSCs and should be preferred over bead sorting. Complex multiparameter panels have been designed for sorting of MDSCs by flow cytometry from human tumor samples of colorectal cancer[19–21], hepatocellular carcinoma[22,23], head and neck cancer[24] or gastric cancer[25], which included CD33, CD11b, HLA-DR, CD15 and CD14 as markers and could even distinguish between M- and PMN-MDSCs. While FACS offers higher precision, it can be time-consuming and expensive, and its prolonged processing times can negatively affect cell viability and functionality[29]. In addition, FACS requires sophisticated instrumentation and skilled personnel, limiting its accessibility in resource-constrained settings. Considering MACS approach, it is not easily compatible with multiple-marker profile and can lack specificity when dealing with heterogeneous populations such as MDSCs, since these cells may express the target marker at low levels, leading to incomplete enrichment or exclusion. Nevertheless, when processing multiple samples, MACS is faster due to its ability to run samples in parallel[32].

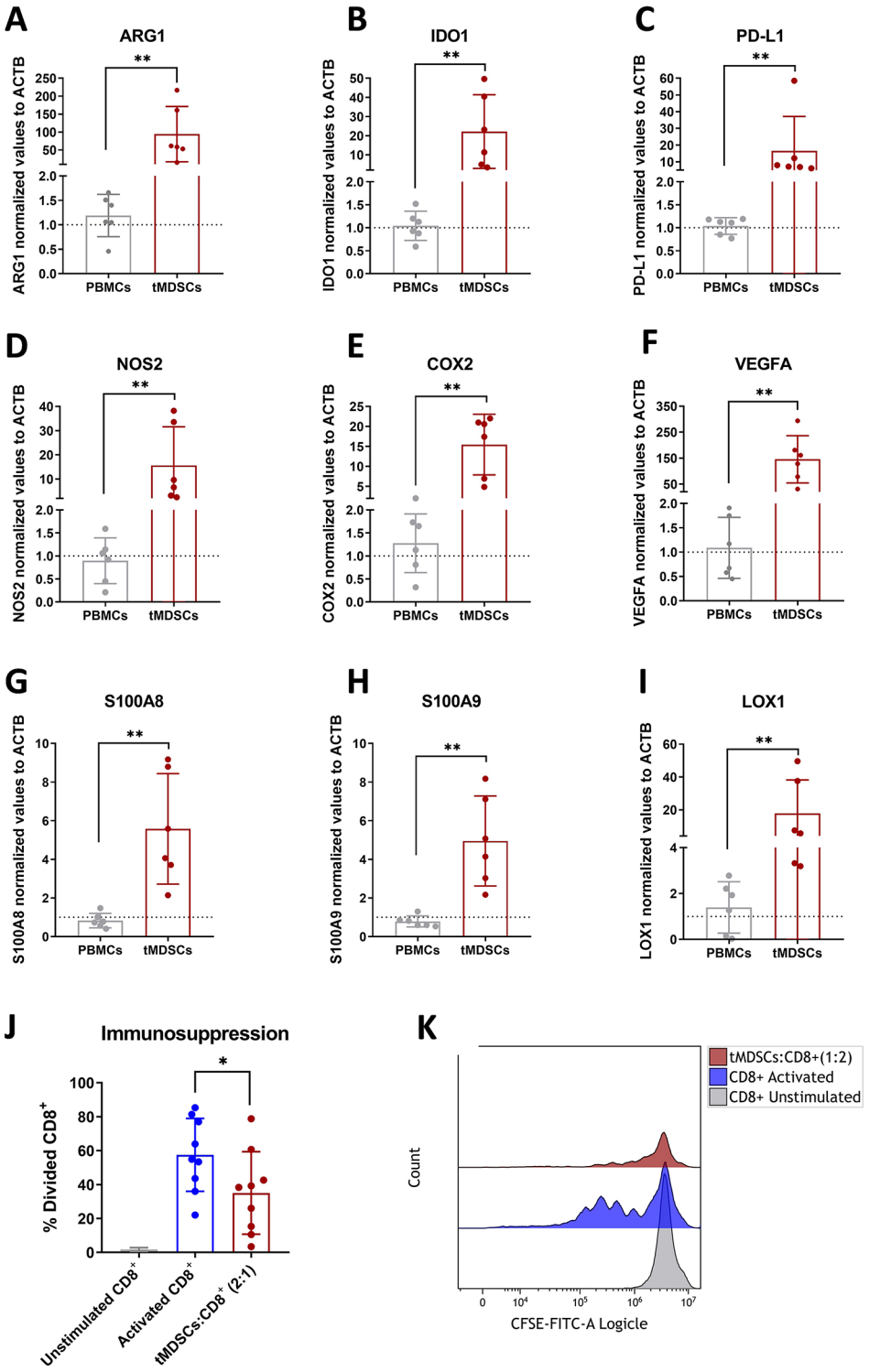

Fig. 3. Functional assays for tMDSCs characterization. *ARG1* (**A**), *IDO1* (**B**), *PD-L1* (**C**), *NOS2* (**D**), *COX2* (**E**), *VEGFA* (**F**), *S100A8* (**G**), S100A9 (**H**) and *LOX1* (**I**) relative gene expression levels in tumor-infiltrating MDSCs (n = 6). Values were mean ± SD, $^{**}p < 0.01$ determined by Mann–Whitney test. (**J**) Inhibitory effect of tMDSCs on proliferation of $CD8^+$ T cells. Data are representative of 6 independent experiments. Values were mean ± SD, $^{*}p < 0.05$ determined by One-Way ANOVA. (**K**) Representative flow histograms from experiments in (**J**).

An example of a magnetic bead only isolation protocol from human lung biopsy specimens was conducted using the anti-CD14 and anti-CD11b MACS magnetic sorting system to isolate tumor-infiltrating PMN- and Mo-MDSCs[18]. Due to the similar immunophenotypic markers between PMN- and M-MDSCs and neutrophils and monocytes, respectively, flow cytometry should not be the unique method employed for MDSCs characterization

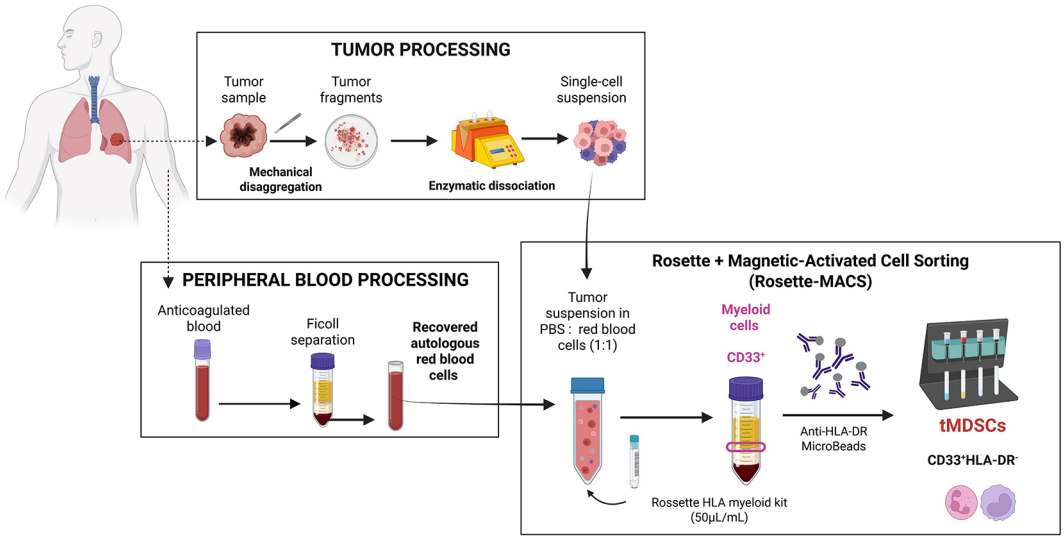

Fig. 4. Flow chart for the isolation of tMDSCs by combining RosetteSep and MACS technologies.

and functional assays are highly recommendable for confirming their functionality (e.g., immunosuppressive activity). The almost universal standards to assess MDSCs suppressive activity are T cell proliferation and cytokine release assays[33]. The proliferation of T cells is assessed through either the dilution of a tracking dye such as carboxyfluorescein succinimidyl ester (CFSE) or through tritiated thymidine incorporation. Suppression of cytokine production is assessed by ELISA using the supernatant of the co-incubation. IFNγ is the most common effector cytokine tested. Other cytokines of interest include IL-10, IL-2 or TGF-β. Moreover, *ARG1*, *IDO1* and *NOS2* expression in MDSCs can be confirmed by qRT-PCR[30].

Here we set out to obtain the population of MDSCs from human NSCLC tumor samples using an innovative approach that is based on the use of RosetteSep technology combined with MACS (Fig. 4 and Supplementary Protocol). Our procedure yields functional cells with higher purities than two of the most used separation techniques (i.e., MACS and FACS) and addresses critical limitations of currently methodologies, which provides a robust platform for obtaining functional MDSCS. Frequently, functional evaluation of isolated MDSCs is overlooked or neglected despite its importance. In our protocol we incorporate the possibility to further characterize the isolated cells in terms of gene expression and immunosuppressive functions as the recovered cells show high viability.

Our study is limited due to the lung tumors being heterologous, as immune cell infiltration levels in the tumor fluctuate among patients, affecting the quantity of tMDSCs recovered by means of our proposed protocol. Moreover, fresh autologous red blood cells are needed in our separation method which could be a restriction in some cases (e.g., poor vein accessibility, dehydration or bleeding disorders). It is worth noting that we have previously tested other options to obtain RBCs which failed to succeed. For instance, we preserved patients' peripheral blood samples at 4ºC for up to 1 week to have a stock and avoid blood sampling for some patients and observed a reduction in RBCs quantity because of hemolysis. We also tried to obtain RBCs after density gradient enrichment with RosetteSep™ HLA Myeloid Cell Enrichment Kit in order to isolate circulating and tumor MDSCs from the same patient, but those recovered RBCs were already crosslinked with antibodies in the kit, so no more immunorosettes could be formed with tumor suspension cells and the number of isolated tMDSC was very low. To continue with the limitations, by means of our methodology, only myeloid subtypes of cells ($CD33^+$) can be enriched as the RosetteSep™ HLA Myeloid Cell Enrichment Kit crosslinks erythrocytes to non-myeloid cells, pelleting them after density gradient centrifugation. By contrast, FACS and MACS give the opportunity to isolate lymphoid cells from tumor biopsies in parallel to tMDSCs. Finally, a common limitation of the three compared methods is preservation of lung tumor biopsies for cell isolation, which is essential to maintain cell integrity and functionality. If the fresh tumor sample is not properly conserved, the yield and viability of isolated tMDSCs may be low, disturbing downstream cell applications.

In conclusion, our results showed the suitability of the combined use of Rosette-MACS to isolate tMDSCs. This unheard-of approach enables the enrichment and further characterization of tMDSCs from human lung biopsies and provides a suitable model to mimic MDSCs-derived immunosuppressive mechanisms within the tumor microenvironment, which provides am experimental framework to search for new therapeutic avenues for NSCLC treatment.

Methods

Resources table

Reagent or resource	Source	Identifier
Antibodies		
FITC anti-human CD33 (clone REA775)	Miltenyi Biotec	Cat #130-111-027
PE anti-human CD11b (clone REA713)	Miltenyi Biotec	Cat #130-110-553
PE-Cy7 anti-human HLA-DR (clone REA805)	Miltenyi Biotec	Cat #130-111-791
Biological samples		
Human non-small cell lung cancer tumor biopsies	Hospital La Ribera, Alzira	See Table S1
Human non-small cell lung cancer peripheral blood	Hospital La Ribera, Alzira	See Table S1
Chemicals, peptides, and recombinant proteins		
DMEM/F-12 medium	Gibco	Cat #31,331-028
Antibiotic–antimycotic	Biowest	Cat #L0010
Phosphate-buffered saline (PBS)	Biowest	Cat #X0515
RosetteSep DM-M density medium	STEMCELL	Cat #15725
Carboxyfluorescein diacetate succinimidyl ester (CFSE)	Life technologies	Cat # C34554
RPMI1640 medium	Biowest	Cat #L0498
Fetal bovine serum (FBS)	Gibco	Cat #A3160502
Critical commercial assays		
Tumor dissociation kit	Miltenyi Biotec	Cat #130-095-929
Anti-HLA-DR Ab-coated magnetic beads	Miltenyi Biotec	Cat #130-046-101
Anti-CD14 Ab-coated magnetic beads	Miltenyi Biotec	Cat #130-050-201
RosetteSep HLA myeloid cell enrichment cocktail	STEMCELL	Cat #15272HLA
E.Z.N.A. total RNA kit	Omega Bio-tek	Cat #R6934-02
PrimeScript RT reagent kit	Takara	Cat #RR037A
SYBR Premix Ex Taq™ DNA Polymerase	Takara	Cat #RR420W
Anti-CD8 Ab-coated magnetic beads	Miltenyi Biotec	Cat #130-045-201
T Cell TransAct	Miltenyi Biotec	Cat #130-111-160
Oligonucleotides		
Primer: ACTB, forward: ACAGAGCCTCGCCTTTGC	Condalab	N/A
Primer: ARG1, forward: CCGTGCCCAGATTCTGACTT	Condalab	N/A
Primer: IDO1, forward: ATGAAGAAGTGGGCTTTGCTCT	Condalab	N/A
Primer: PD-L1, forward: CCTACTGGCATTTGCTGAACG	Condalab	N/A
Primer: NOS2, forward: CTGGATTTGGCTGGTCCCT	Condalab	N/A
Primer: COX2, forward: CTTGCAGTGAGCGTCAGGAG	Condalab	N/A
Primer: VEGFA, forward: TGAGCTTCCTACAGCACAACAA	Condalab	N/A
Primer: S100A8, forward: ATGCCGTCTACAGGGATGAC	Condalab	N/A
Primer: S100A9, forward: CAATACTCTGTGAAGCTGGGG	Condalab	N/A
Primer: LOX1, forward: AGGTCTTCAGTTTCTTTACTCTCC	Condalab	N/A
Software and algorithms		
BD FACSDiva version 8.0.1	BD Biosciences	RRID:SCR_001456
Kaluza analysis version 2.1	Beckman Coulter	RRID:SCR_016182
Prism version 9.2.0	GraphPad Software	RRID:SCR_002798

Patient cohort

The study conforms to the Declaration of Helsinki for use of human tissue or subjects and the study protocols as well as the collection and use of blood samples and tissues were previously approved by Research Ethics Committee for Medicines from the Hospital Universitario y Politécnico La Fe. A written informed consent was taken from all patients prior to blood sampling and/or tumor tissue harvesting. Tumor tissue (TT) and peripheral blood (PB) were obtained from 14 NSCLC patients (#01 to #14) who underwent surgery at Hospital La Ribera, Alzira, Valencia. Demographical details and clinicopathological features of study population are shown in Table S1. These patients were treatment-naïve prior to surgery. Tissue specimens were stored in 20 mL of DMEM/F-12 (1:1) (1X) + GlutaMAX™-I (Invitrogen, Carlsbad, CA) supplemented with 2% Antibiotic–Antimycotic (Biowest, Nuaillé, France). Peripheral blood samples were collected by vein puncture in tubes containing EDTA as anticoagulant. The flow chart for the experimental design and tissue processing is shown in Fig. 1A.

Cell isolation from tumor samples

Fresh tumor tissue from 14 human patients undergoing resection of NSCLC were used. To obtain single cell suspensions from tumors, solid tissues were washed with phosphate-buffered saline (PBS) (Biowest, Nuaillé, France), measured, weighted and cut into small pieces using a surgical scapel. Further enzymatic disaggregation was performed on gentleMACS dissociator (Miltenyi Biotec, Bergisch Gladbach, Germany) combined with

the Tumor Dissociation Kit (Miltenyi Biotec, Bergisch Gladbach, Germany), according to the manufacturer's instructions. The cell suspension was then passed through a 70 μm mesh cell strainer to remove debris and aggregates.

Isolation of tumor-infiltrating myeloid-derived suppressor cells (tMDSCs)

Fluorescence-activated cell sorting (FACS)

#01, #02, #03 and #04 Cells isolated from tumor tissues were resuspended in flow cytometry staining buffer (PBS with 0.5% BSA and 2 mM EDTA). Cells were then stained with the following cell surface antibodies: CD33-fluorescein isothiocyanate (clone REA775; Miltenyi Biotec, Bergisch Gladbach, Germany), CD11b-phycoerythrin (clone REA713; Miltenyi Biotec, Bergisch Gladbach, Germany) and HLA-DR-phycoerythrin-Cy7 (clone REA805; Miltenyi Biotec, Bergisch Gladbach, Germany) and incubated at 4 °C for 10 min. For cell sorting, BD FACSAria III SORP cell sorter was utilized with BD FACSDiva software (BD Biosciences). Purities of the sorted population were always checked and confirmed. Kaluza Analysis Version 2.1 (Beckman Coulter, Brea, USA) was used for data analyses.

Magnetic-activated cell sorting (MACS)

#05, #06, #07 and #08 Freshly obtained tumor cell suspensions were applied for the enrichment of HLA-DR$^-$CD14$^+$ tMDSCs using MACS magnetic bead isolation kits (Miltenyi Biotec, Bergisch Gladbach, Germany) according to the manufacturer's instructions. In brief, isolated cells were incubated with anti-HLA-DR Ab-coated magnetic beads (Miltenyi Biotec, Bergisch Gladbach, Germany) for 15 min in the refrigerator (2 – 8 °C). Following incubation time, the cells were washed by adding 2 mL of buffer per 10^7 cells and centrifuged at 500 × g for 5 min and resultant pellets were resuspended in buffer. Then, the cell suspension was applied onto an appropriate MACS Column and MACS Separator (Miltenyi Biotec, Bergisch Gladbach, Germany). Negatively selected cells (HLA-DR$^-$) were then incubated with anti-CD14 Ab-coated magnetic beads Separator (Miltenyi Biotec, Bergisch Gladbach, Germany) for 15 min to identify HLA-DR$^-$CD14$^+$ cells positively. Finally, the cells were tested for purity.

RosetteSep™ HLA myeloid cell enrichment kit + magnetic-activated cell sorting (MACS): Rosette-MACS

#09, #10, #11, #12, #13 and #14 A Ficoll-Hypaque density gradient centrifugation was performed to separate autologous red blood cells present in fresh peripheral blood samples. These cells were put together with the cell suspension obtained from tumor dissociation, after centrifugation and resuspension in PBS, so that the proportion of red blood cells:tumor suspension in PBS is 1:1. After that, RosetteSep HLA Myeloid Cell Enrichment Cocktail (Stemcell, Saint Égrève, France) was added at 50 μL/mL of cell suspension and incubated for 20 min at room temperature. The mixture was then layered on top of 15 mL of RosetteSep DM-M Density Medium (Stemcell, Saint Égrève, France) and centrifuged at 1200 × g for 20 min with the brake off to enrich the population of CD33$^+$ myeloid cells. Cells were then washed with PBS + 2% FBS and erythrocytes were removed by hypotonic lysis. Finally, cells were labelled with HLA-DR antibodies conjugated to magnetic beads (Miltenyi Biotec, Bergisch Gladbach, Germany) and the negative fraction (HLA-DR$^-$ cells) was enriched using a LS column, according to the manufacturer's instructions. The obtained cells (CD33$^+$HLA-DR$^-$, named as tMDSCs) were further characterized.

The flow chart for the isolation of tMDSCs by combining RosetteSep technique and MACS technology is shown in Fig. 4**.**

Characterization of tumor-infiltrating myeloid-derived suppressor cells (tMDSCs)

Flow cytometry

The phenotype of tumor-infiltrating MDSCs was determined by multi-colour flow cytometry using the following antibodies: anti-CD11b (clone REA713), anti-CD33 (clone REA775) and anti-HLA-DR (clone REA805). Antibodies were purchased from Miltenyi Biotec. Dead cells were excluded based on the forward and side scatter. For each sample, at least 10,000 events were recorded. Samples were acquired using a CytoFlex S (Beckman Coulter, Brea, USA) and data was analysed using Kaluza Analysis Version 2.1 (Beckman Coulter, Brea, USA).

Gene expression analysis

Total RNA was extracted from tMDSCs using E.Z.N.A. Total RNA Kit (Omega Bio-tek, Norcross, GA) according to the manufacturer's instructions. The concentration of RNA was determined using a spectrophotometer. For mRNA detection, cDNA was synthesized by reverse transcription with PrimeScript RT Reagent Kit (Perfect Real Time) (Takara, Japan) and according to the manufacturer's instructions. The real-time PCR reaction contained SYBR Premix Ex Taq™ DNA Polymerase (Perfect Real Time) (Takara, Japan) and the following primers: *ACTB*, 5'-ACAGAGCCTCGCCTTTGC-3'; *ARG1*, 5'-CCGTGCCCAGATTCTGACTT-3'; *IDO1*, 5'-ATGAAGAAG TGGGCTTTGCTCT-3'; *PD-L1*, 5'-CCTACTGGCATTTGCTGAACG-3'; *NOS2*, 5'-CTGGATTTGGCTGGT CCCT-3'; *COX2*, 5'- CTTGCAGTGAGCGTCAGGAG-3'; *VEGFA*, 5'-TGAGCTTCCTACAGCACAACAA-3'; *S100A8,* 5'- ATGCCGTCTACAGGGATGAC-3'; S100A9, 5'-CAATACTCTGTGAAGCTGGGG-3' and LOX1, 5'- AGGTCTTCAGTTTCTTTACTCTCC-3'. qPCR was performed in duplicate for each sample. The program of two step real time RT-PCR was retro transcription at 37 °C for 15 min, followed by warming at 50 °C for 2 min, denaturation at 95 °C for 1 min, 40 cycles of amplification at 95 °C for 15 s and 60 °C for 35 s and melting at 95 °C for 15 s, 60 °C for 1 min and 95 °C for 15 s. Expression levels of the genes were normalized to that of internal control β-actin by using the $2^{-\Delta\Delta Ct}$ cycle threshold method. Fold expression was calculated relative to PBMCs isolated from healthy controls by Ficoll-Hypaque density gradient centrifugation.

In vitro proliferation assays

Responder $CD8^+$ T cells were purified from buffy coats isolated from healthy donors using anti-CD8 Ab-coated magnetic beads (Miltenyi Biotec, Bergisch Gladbach, Germany). $CD8^+$ T cells were labelled with 2.5 µM carboxyfluorescein diacetate succinimidyl ester (CFSE; Life Technologies) in PBS for 20 min at 37 °C and washed once with RPMI supplemented with FBS to remove excess CFSE. CFSE-labelled $CD8^+$ T cells were non-specifically activated with soluble anti-CD3/CD28 (T cell TransAct; Miltenyi Biotec, Bergisch Gladbach, Germany) and co-cultured at 1:2 ratios of $CD8^+$ T cells to tMDSCs (responder cells). $CD8^+$ T cells with or without T Cell TransAct stimulation was used as positive or negative control, respectively. After 4 days of co-culture in 5% CO2 incubator at 37 °C, $CD8^+$ T cell proliferation was assessed by analysing CFSE dilution by flow cytometry using a CytoFlex S (Beckman Coulter, Brea, USA). Dead cells were gated out by particle size on the FSC vs SSC density plot. The percentages of proliferating cells were determined and calculated by Kaluza Analysis Version 2.1 (Beckman Coulter, Brea, USA).

Statistical analysis

Statistical analysis was performed using GraphPad Prism (Version 9.2.0). Data were expressed as mean ± SD for quantitative measures and both number and percentage for categorised data. The Mann–Whitney test was used for comparison between two independent groups for non-parametric data and One-Way ANOVA was used when more than two independent groups were compared. A p value < 0.05 indicated statistical significance while $p < 0.01$ and 0.001 indicated high statistical significance.

Data availability

This paper does not report original code. Any additional information required to reanalyze the data reported in this paper is available from the corresponding author upon request.

Received: 14 January 2025; Accepted: 23 April 2025
Published online: 30 April 2025

References

1. Rashid, M. H. et al. Critical immunosuppressive effect of MDSC-derived exosomes in the tumor microenvironment. *Oncol. Rep.* **45**(3), 1171–1181 (2021).
2. Elpek, K. G. et al. The tumor microenvironment shapes lineage, transcriptional, and functional diversity of infiltrating myeloid cells. *Cancer Immunol. Res.* **2**(7), 655–667 (2014).
3. Motallebnezhad, M. et al. The immunobiology of myeloid-derived suppressor cells in cancer. *Tumour Biol. J. Int. Soc. Oncodev. Biol. Med.* **37**(2), 1387–1406 (2016).
4. Bleve, A., Durante, B., Sica, A. & Consonni, F. M. Lipid metabolism and cancer immunotherapy: Immunosuppressive myeloid cells at the crossroad. *Int. J. Mol. Sci.* **21**(16), 5845 (2020).
5. Hammami, I. et al. Immunosuppressive activity enhances central carbon metabolism and bioenergetics in myeloid-derived suppressor cells in vitro models. *BMC Cell Biol.* **13**, 18 (2012).
6. Li, X. et al. Metabolic reprogramming of myeloid-derived suppressor cells: An innovative approach confronting challenges. *J. Leukoc. Biol.* **110**(2), 257–270 (2021).
7. Hofer, F. et al. A complex metabolic network confers immunosuppressive functions to myeloid-derived suppressor cells (MDSCs) within the tumour microenvironment. *Cells* **10**(10), 2700 (2021).
8. Casacuberta-Serra, S. et al. Myeloid-derived suppressor cells can be efficiently generated from human hematopoietic progenitors and peripheral blood monocytes. *Immunol. Cell Biol.* **95**(6), 538–548 (2017).
9. Gabrilovich, D. I. Myeloid-derived suppressor cells. *Cancer Immunol. Res.* **5**(1), 3–8 (2017).
10. Lakshmanachetty, S., Cruz-Cruz, J., Hoffmeyer, E., Cole, A. P. & Mitra, S. S. New insights into the multifaceted role of myeloid-derived suppressor cells (MDSCs) in high-grade gliomas: From metabolic reprograming, immunosuppression, and therapeutic resistance to current strategies for targeting MDSCs. *Cells* **10**(4), 893 (2021).
11. Cresswell, G. M. et al. Folate receptor beta designates immunosuppressive tumor-associated myeloid cells that can be reprogrammed with folate-targeted drugs. *Can. Res.* **81**(3), 671–684 (2021).
12. Hossain, F. et al. Inhibition of fatty acid oxidation modulates immunosuppressive functions of myeloid-derived suppressor cells and enhances cancer therapies. *Cancer Immunol. Res.* **3**(11), 1236–1247 (2015).
13. Yamauchi, Y. et al. Circulating and tumor myeloid-derived suppressor cells in resectable non-small cell lung cancer. *Am. J. Respir. Crit. Care Med.* **198**(6), 777–787 (2018).
14. Yang, Z. et al. Myeloid-derived suppressor cells-new and exciting players in lung cancer. *J. Hematol. Oncol.* **13**(1), 10 (2020).
15. Li, Y. et al. Novel characterization of myeloid-derived suppressor cells in tumor microenvironment. *Front. Cell Dev. Biol.* **9**, 698532 (2021).
16. Lin, S. et al. Myeloid-derived suppressor cells promote lung cancer metastasis by CCL11 to activate ERK and AKT signaling and induce epithelial-mesenchymal transition in tumor cells. *Oncogene* **40**(8), 1476–1489 (2021).
17. Lechner, M. G. et al. Functional characterization of human Cd33+ and Cd11b+ myeloid-derived suppressor cell subsets induced from peripheral blood mononuclear cells co-cultured with a diverse set of human tumor cell lines. *J. Transl. Med.* **9**, 90 (2011).
18. Li, J. et al. CD39/CD73 upregulation on myeloid-derived suppressor cells via TGF-β-mTOR-HIF-1 signaling in patients with non-small cell lung cancer. *Oncoimmunology* **6**(6), e1320011 (2017).
19. Saleh, R. et al. RNA-Seq analysis of colorectal tumor-infiltrating myeloid-derived suppressor cell subsets revealed gene signatures of poor prognosis. *Front. Oncol.* **10**, 604906 (2020).
20. Sasidharan Nair, V. et al. Transcriptomic profiling disclosed the role of DNA methylation and histone modifications in tumor-infiltrating myeloid-derived suppressor cell subsets in colorectal cancer. *Clin. Epigenet.* **12**(1), 13 (2020).
21. Wang, Y. et al. Granulocytic myeloid-derived suppressor cells promote the stemness of colorectal cancer cells through exosomal S100A9. *Adv. Sci.* **6**(18), 1901278 (2019).
22. Zhou, J. et al. Hepatoma-intrinsic CCRK inhibition diminishes myeloid-derived suppressor cell immunosuppression and enhances immune-checkpoint blockade efficacy. *Gut* **67**(5), 931–944 (2018).
23. Baumann, T. et al. Regulatory myeloid cells paralyze T cells through cell-cell transfer of the metabolite methylglyoxal. *Nat. Immunol.* **21**(5), 555–566 (2020).
24. Corzo, C. A. et al. HIF-1α regulates function and differentiation of myeloid-derived suppressor cells in the tumor microenvironment. *J. Exp. Med.* **207**(11), 2439–2453 (2010).

25. Moaaz, M., Lotfy, H., Elsherbini, B., Motawea, M. A. & Fadali, G. TGF-β enhances the anti-inflammatory effect of tumor-infiltrating CD33+11b+HLA-DR myeloid-derived suppressor cells in gastric cancer: A possible relation to MicroRNA-494. *Asian Pac. J. Cancer Prev. APJCP* **21**(11), 3393–3403 (2020).
26. Lang, S. et al. Clinical relevance and suppressive capacity of human myeloid-derived suppressor cell subsets. *Clin. Cancer Res. Off. J. Am. Assoc. Cancer Res.* **24**(19), 4834–4844 (2018).
27. Duarte-Sanmiguel, S. et al. Guided migration analyses at the single-clone level uncover cellular targets of interest in tumor-associated myeloid-derived suppressor cell populations. *Sci. Rep.* **10**(1), 1189 (2020).
28. Stiff, A. et al. Myeloid-derived suppressor cells express Bruton's tyrosine kinase and can be depleted in tumor-bearing hosts by ibrutinib treatment. *Cancer Res.* **76**(8), 2125–2136 (2016).
29. Pfister, G., Toor, S. M., Sasidharan Nair, V. & Elkord, E. An evaluation of sorter induced cell stress (SICS) on peripheral blood mononuclear cells (PBMCs) after different sort conditions - Are your sorted cells getting SICS?. *J. Immunol. Methods* **487**, 112902 (2020).
30. Bruger, A. M. et al. How to measure the immunosuppressive activity of MDSC: Assays, problems and potential solutions. *Cancer Immunol. Immunother. CII* **68**(4), 631–644 (2019).
31. Kumar, V., Patel, S., Tcyganov, E. & Gabrilovich, D. I. The nature of myeloid-derived suppressor cells in the tumor microenvironment. *Trends Immunol.* **37**(3), 208–220 (2016).
32. Sutermaster, B. A. & Darling, E. M. Considerations for high-yield, high-throughput cell enrichment: Fluorescence versus magnetic sorting. *Sci. Rep.* **9**(1), 227 (2019).
33. Bronte, V. et al. Recommendations for myeloid-derived suppressor cell nomenclature and characterization standards. *Nat. Commun.* **7**, 12150 (2016).

Acknowledgements

This work is supported by the Carlos III Institute of Health of the Spanish Ministry of Science, Innovation and Universities (PI23/01369 and PI20/00580) and Conselleria de Innovación, Universidades, Ciencia y Sociedad Digital (CIAICO/2022/251) to A.L. This research was also supported by the Spanish Ministry of Ministry of Science, Innovation and Universities through the FPU fellowship program (Formación de Profesorado Universitario) under grant number FPU18/02951 to M.P.

Author contributions

A.L conceived this study and orchestrated the project. M.B and M.P designed the experiments and conducted the setup of the flow cytometry method for NSCLC patient immunophenotyping. J.G and M.E performed patients´ thoracic surgery, submitted tissue to anatomical pathology and managed participant information with O.J. A.C performed tissue histological and immunohistochemical characterization sample analysis and preparation for subsequent cell isolation. M.P and M.B performed the data analysis and organized the generation of graphic illustrations. J.G. and J.C provided conceptual inputs and supervised patient data. All the authors critically read and commented on the final version of the paper.

Declarations

Competing interests

The authors declare no competing interests.

Additional information

Supplementary Information The online version contains supplementary material available at https://doi.org/10.1038/s41598-025-99877-x.

Correspondence and requests for materials should be addressed to A.L.

Reprints and permissions information is available at www.nature.com/reprints.

Publisher's note Springer Nature remains neutral with regard to jurisdictional claims in published maps and institutional affiliations.